

Supplementary materials

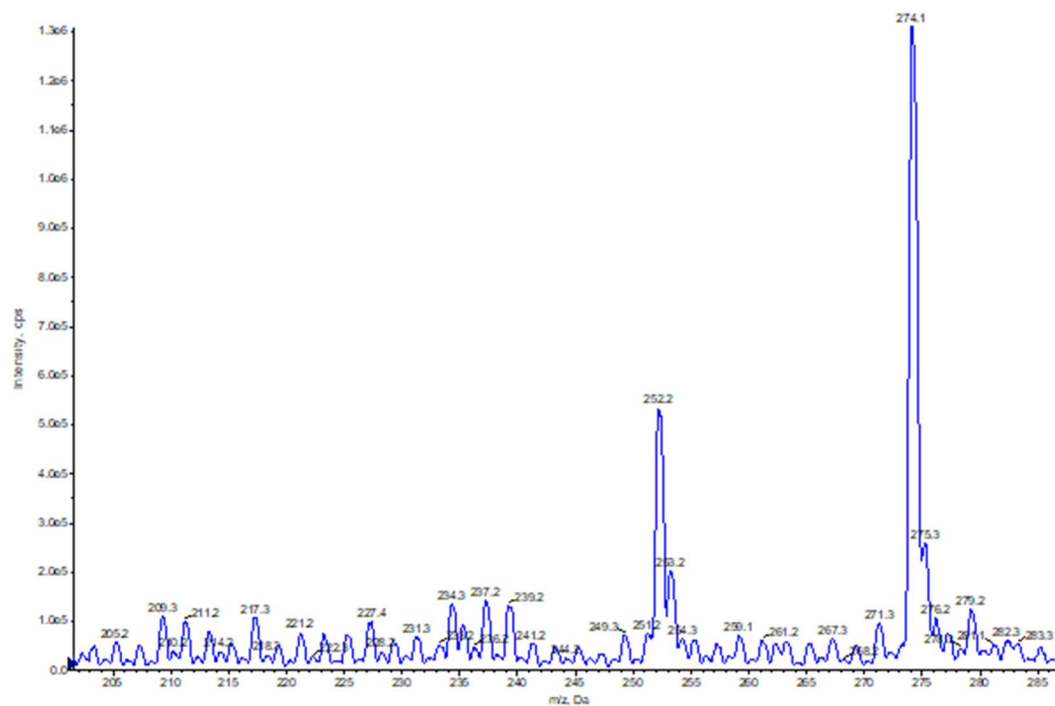


Figure S1. +Q1 mode (without fragmentation)

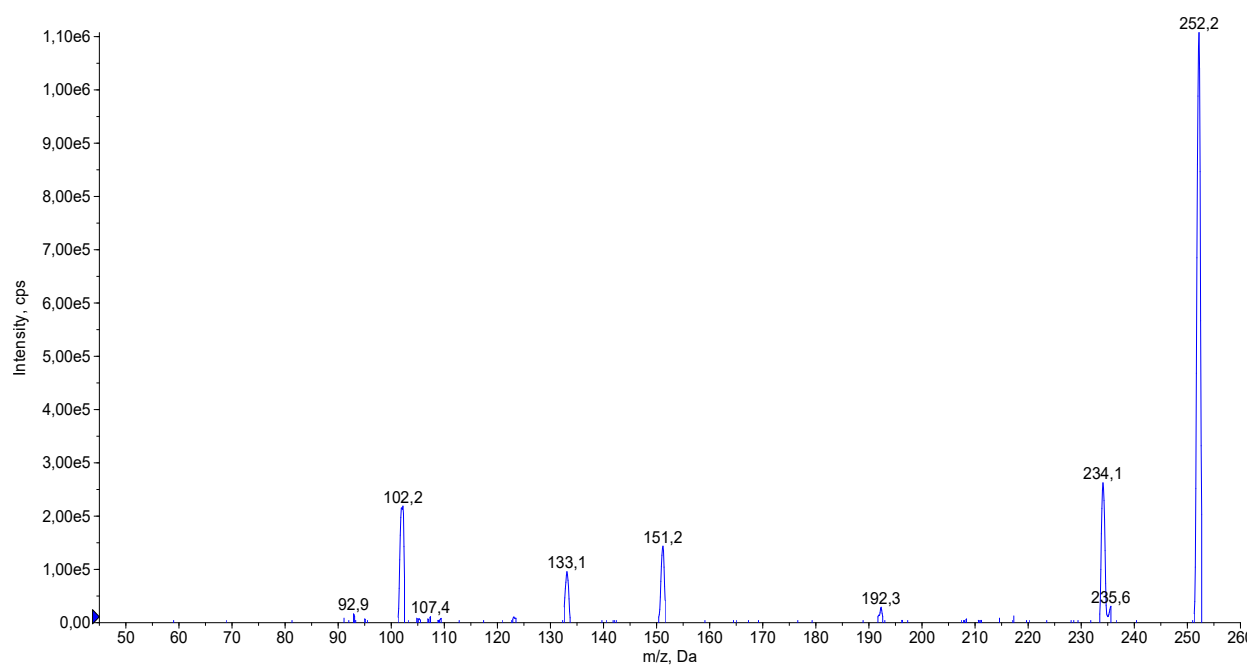


Figure S2. Fragmentation mass spectrum of the protonated form $[M+H]^+$ with $m/z=252.1$ at low energy (CE = 5 V)

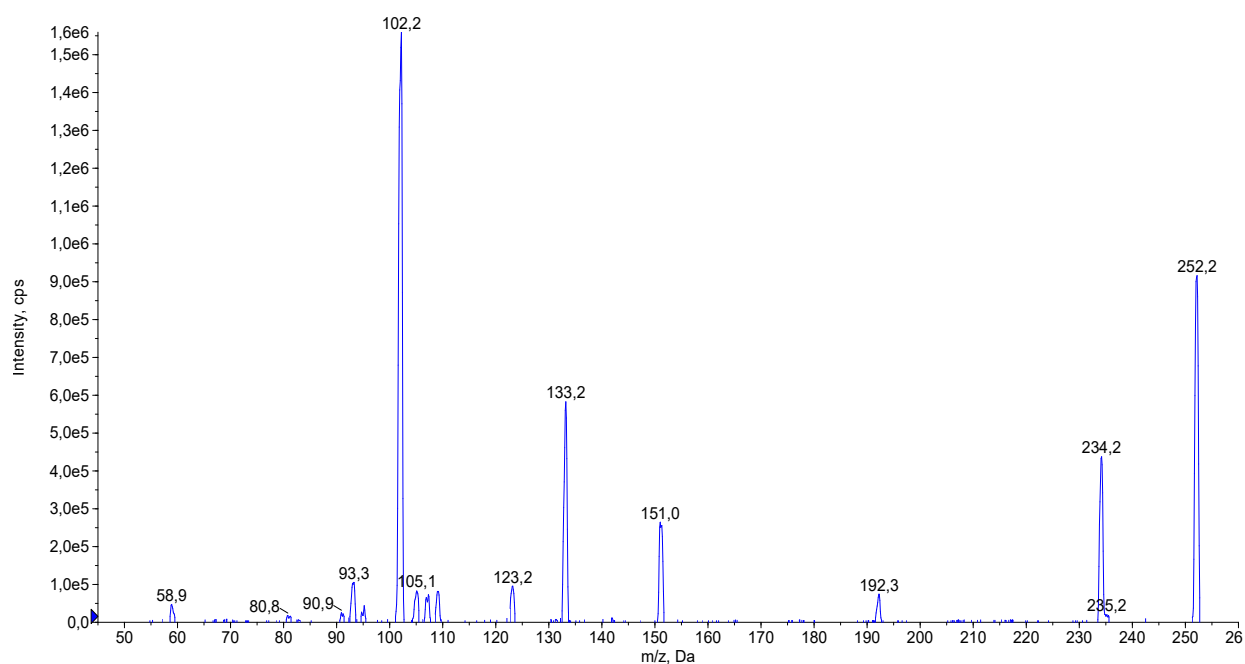


Figure S3. Fragmentation mass spectrum of the protonated form $[M+H]^+$ with $m/z=252.1$ at medium energy (CE = 15 V).

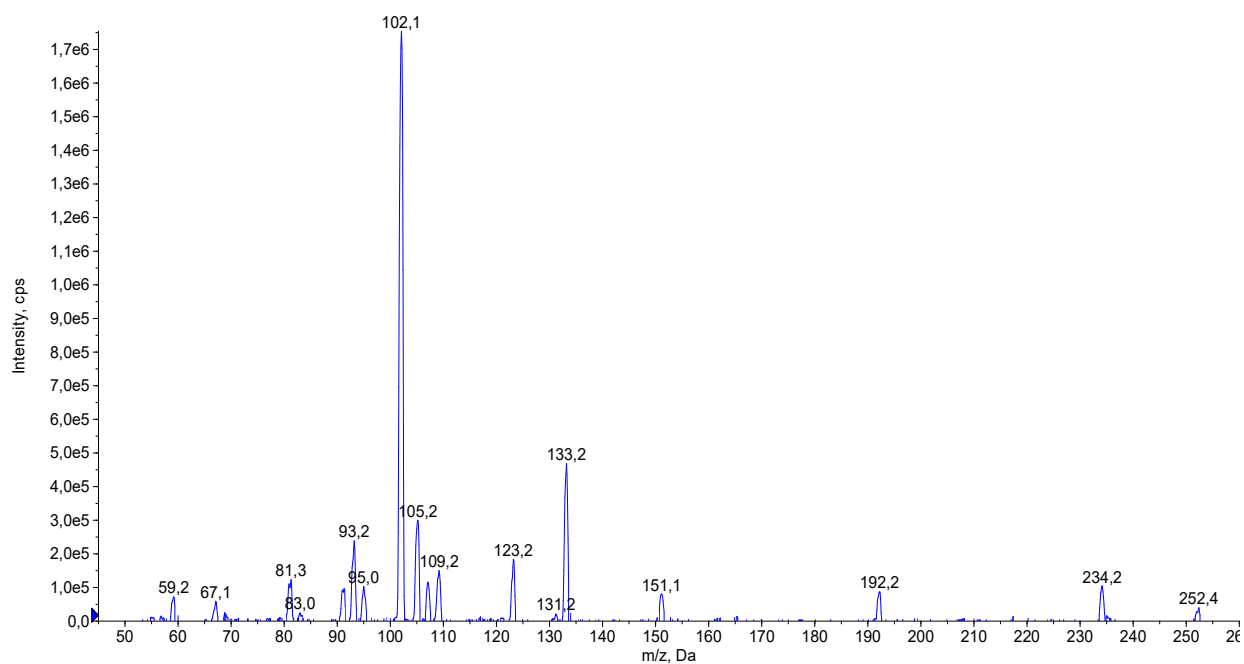


Figure S4. Fragmentation mass spectrum of the protonated form $[M+H]^+$ with $m/z=252.1$ at high energy (CE = 25 V).

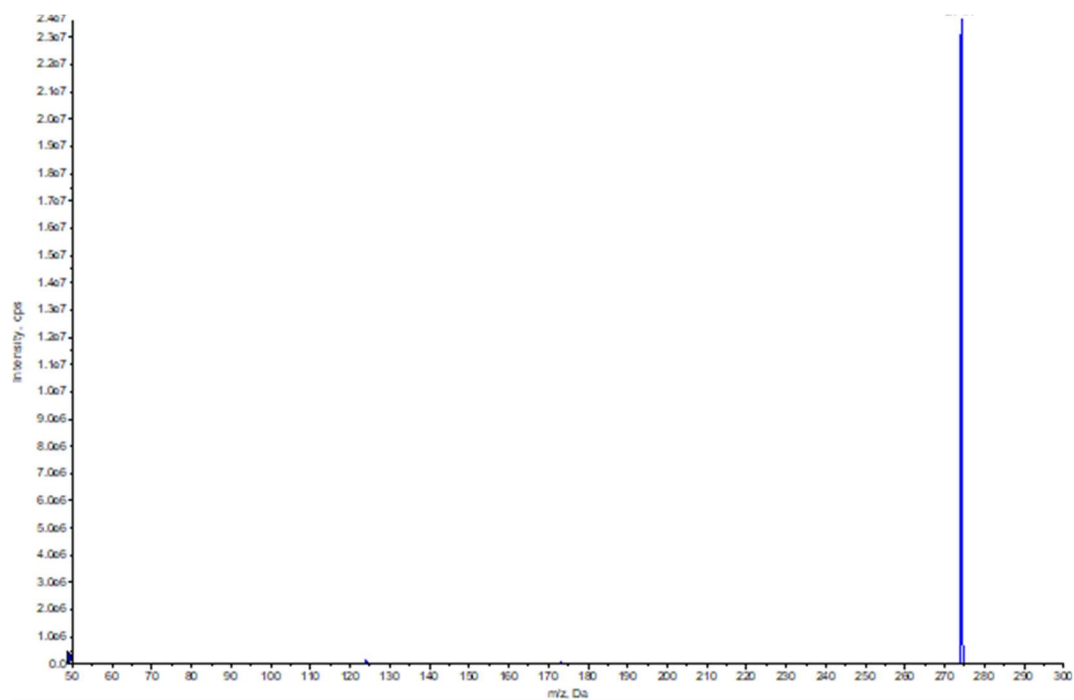


Figure S5. Fragmentation mass spectrum of the adduct $[M+Na]^+$ with $m/z=274.1$ at low energy (CE = 5 V)

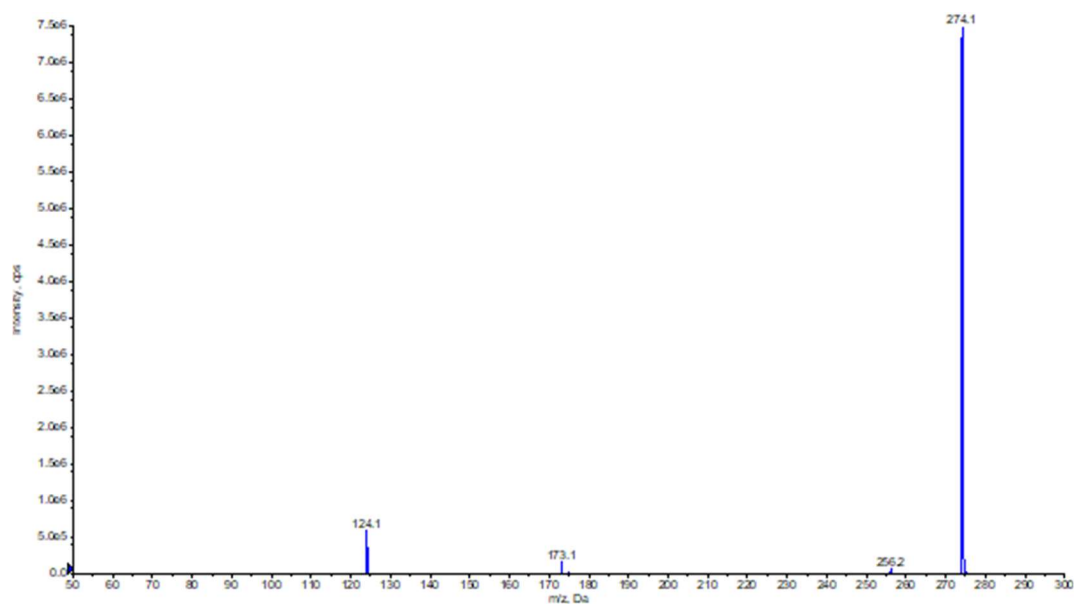


Figure S6. Fragmentation mass spectrum of the adduct $[M+Na]^+$ with $m/z=274.1$ at medium energy (CE = 15 V)

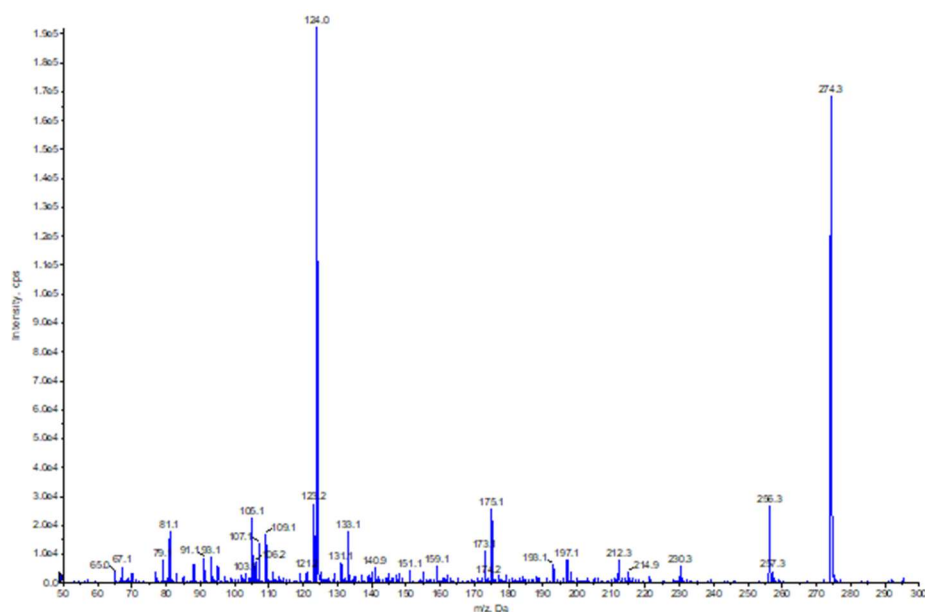


Figure S7. Fragmentation mass spectrum of the adduct $[M+Na]^+$ with $m/z=274.1$ at medium energy (CE = 25 V)

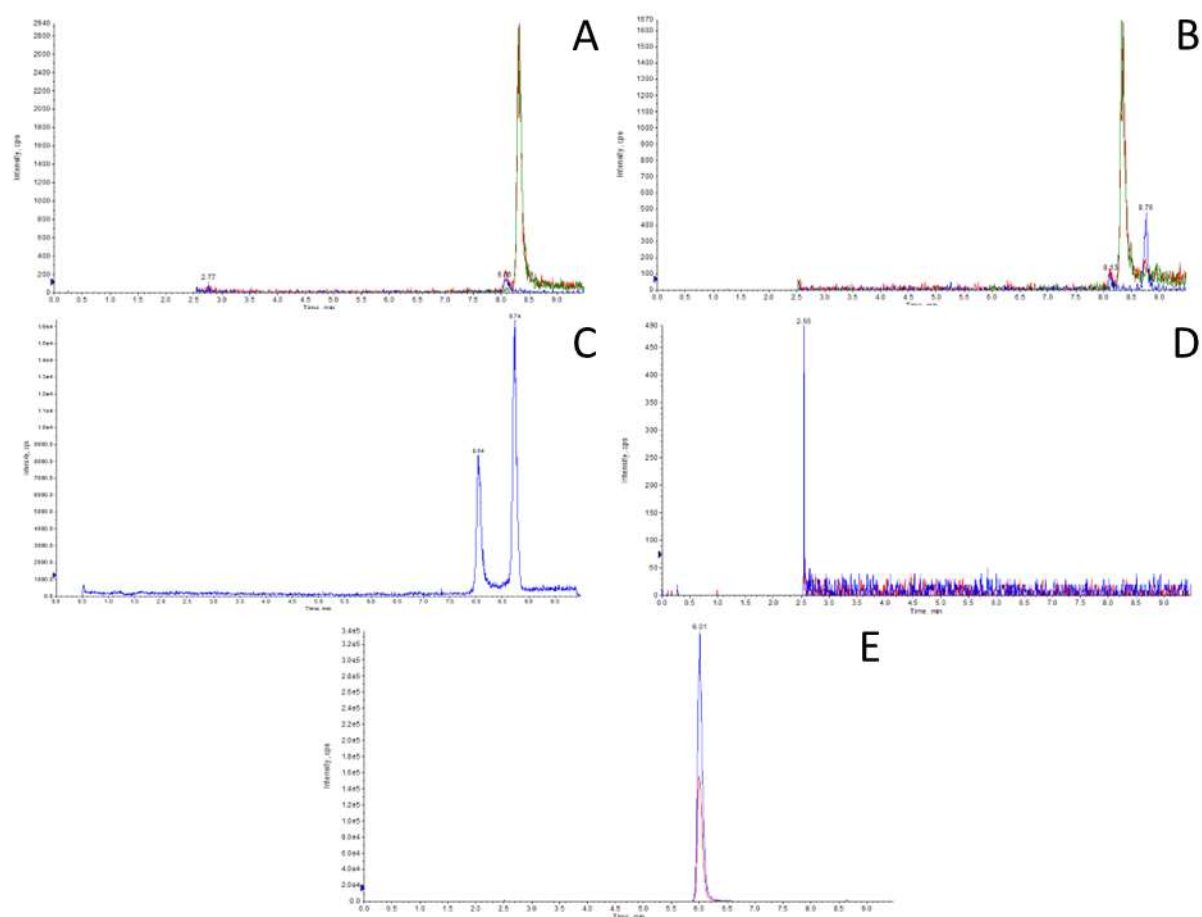


Figure S8. Chromatograms of PA-96 transitions (m/z 252.2→102.1/133.1/151.2) of blank blood (A) and LLOQ sample (B). Extracted ion chromatogram of PA-96 of the transition 252.2→102.1 (C). Chromatograms of 2-Ad (m/z 152.3→93.1/107.2) in blank blood (D) and the LLOQ sample (E).

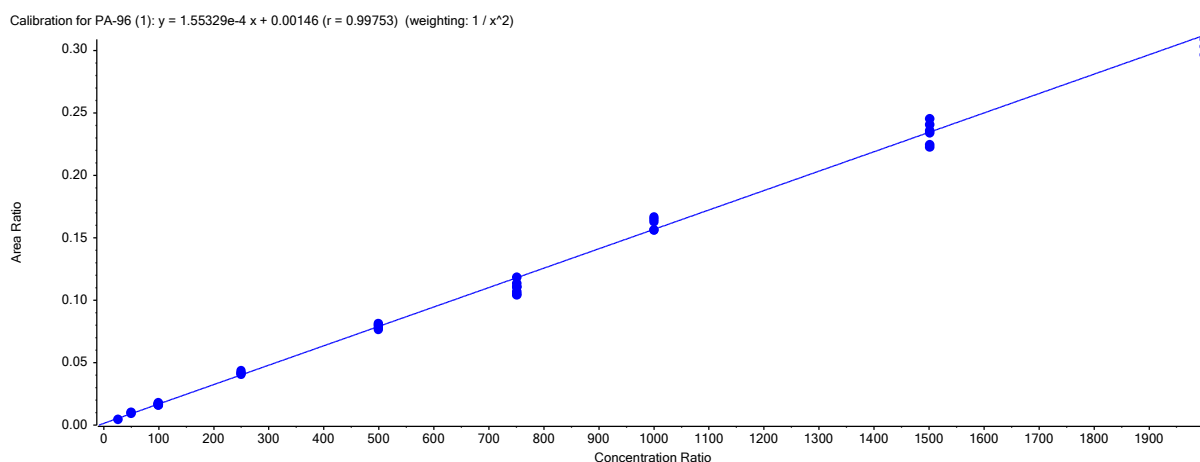


Figure S9 Calibration curve in the range of 25-2000 ng/mL

Table S1. Recovery and matrix effect values

QC sample (ng/mL)	Mean recovery \pm SD, %	Matrix factor \pm SD
LLOQ (25)	53 \pm 4	0.70 \pm 0.03
HQC (1500)	69.5 \pm 1.2	0.448 \pm 0.013

*SD – standard deviation

Table S2. Accuracy and precision for PA-96 quantified in the range of 25-2000 ng/mL.

	LLOQ 25 ng/mL		Low 75 ng/mL		Medium 750 ng/mL		High 1500 ng/mL	
	%nominal \pm SD*	%Er**	%nominal \pm SD	%Er	%nominal \pm SD	%Er	%nominal \pm SD	%Er
Day 1	97 \pm 3	-3.1	99 \pm 4	-0.80	112 \pm 3	+12	112 \pm 4	+12
Day 2	73 \pm 11	-27	101 \pm 4	+1.0	94 \pm 4	-5.7	88.6 \pm 2.1	-11
Day 3	88.7 \pm 2.5	-11	88 \pm 6	-12	112 \pm 3	+12	90.1 \pm 2.1	-9.9
Inter-day	86 \pm 6	-14	96 \pm 5	-4.0	106 \pm 3	+6.0	97.0 \pm 2.7	-3.0

*SD – standard deviation, %

**Er – percentage relative error

Calibration for PA-96 (1): $y = -2.70250\text{e-}9 x^2 + 2.74051\text{e-}4 x - 0.01536$ ($r = 0.99701$) (weighting: $1 / x^2$)

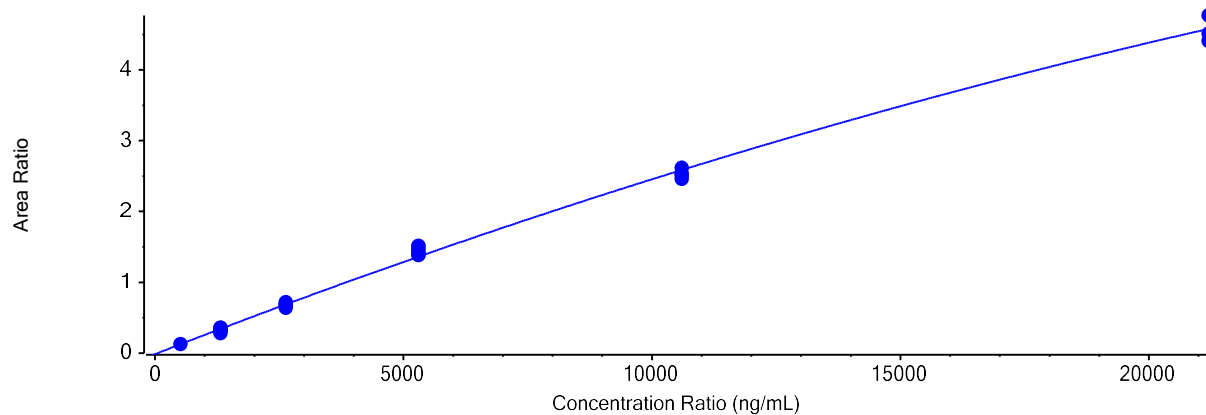


Figure S10. Calibration curve, where x – PA-96 concentration in blood,
Y – the ratio of PA-96/IS in 0.9-21200 ng/mL range

Table S3. Accuracy and precision calculated for the high-concentration range calibration curve

Quality control sample and concentration (ng/mL)	Accuracy, %	CV, %
LLOQ (530)	100.5	4.2
QCL (1760)	95.7	4.4
QCM (8800)	96.2	3.9
QCH (17100)	98.5	11.6

Table S4. Pharmacokinetic parameters of PA-96 after p.o and i.v. administration to mice at different doses and regimens, *mean* \pm *SEM*

PK parameter and dose	Single <i>p.o.</i>		Double <i>p.o.</i> (2 \times 5 mg/kg)		Single i.v. injection	
	5 mg/kg (n=4)	10 mg/kg (n=4)	1 st (n=6)	2 nd (n=6)	1 mg/kg (n=6)	10 mg/kg (n=3)
T _{max} , min	6.3 \pm 1.3	8.8 \pm 1.3	10.0 \pm 2.2	248.3 \pm 2.5	3.3 \pm 0.3	3
C _{max} , ng/mL	36 \pm 8	588 \pm 71	60 \pm 15	58 \pm 13	(3.9 \pm 0.3) \times 10 ²	(7 \pm 3) \times 10 ³
t _{1/2} , min	44 \pm 13	15.2 \pm 1.2	21 \pm 4	19 \pm 3	37 \pm 10	26.1 \pm 2.9
AUC _{0-t} , ng/mL*min	(1.7 \pm 0.3) \times 10 ³	(1.8 \pm 0.4) \times 10 ⁴	(1.5 \pm 0.3) \times 10 ³	(8.1 \pm 2.3) \times 10 ³	(5.1 \pm 0.6) \times 10 ³	(1.3 \pm 0.7) \times 10 ⁵
Vz/F _{obs} , (mg)/(ng/mL)	(1.9 \pm 0.5) \times 10 ⁻¹	(13.7 \pm 2.7) \times 10 ⁻³	0.108 \pm 0.025	0.025 \pm 0.004	(1.1 \pm 0.4) \times 10 ⁻²	(0.40 \pm 0.24) \times 10 ⁻²
Cl/F _{obs} , (mg)/(ng/mL)/min	(3.3 \pm 0.7) \times 10 ⁻³	(6.4 \pm 1.5) \times 10 ⁻⁴	(4.0 \pm 0.8) \times 10 ⁻³	(0.79 \pm 0.14) \times 10 ⁻³	(2.01 \pm 0.19) \times 10 ⁻⁴	(0.10 \pm 0.05) \times 10 ⁻³